Limnol. Oceanogr., 51(4), 2006, 1935–1939

High-frequency internal waves in the littoral zone of a large lake

Abstract—Observations in the littoral zone of a large lake (Lake Constance) revealed strong and periodic fluctuations of temperature and current velocity on timescales between 10 and 15 min associated with high-frequency internal waves. The peak in the spectral energy of the current velocity fluctuations associated with high-frequency internal waves follows the seasonal dynamics of stratification, described by the stability frequency N. A comparison between the nearshore current velocity measurements in the littoral zone with temperature measurements in the pelagic of Lake Constance revealed a strong coupling between the occurrence of high-frequency internal waves in the littoral zone and the passage of the basin-scale internal Kelvin wave with a period of about 4 d.

The littoral zone of a lake, which is usually defined as the shallow area near the shore where light penetration is sufficient for the growth of plants, is an extremely dynamic habitat where the physical conditions are highly variable on diurnal and subdiurnal timescales. Surface waves and the daily meteorological cycle are the most obvious physical processes causing a high temporal variability in the current field and in the thermal regime, particularly in the shallow littoral zone with depths of about 1 m. Here, we present data from Lake Constance demonstrating that current velocities and temperature in the deeper littoral zone, down to a depth of about 20 m, also have a high temporal variability on timescales of minutes to hours, and that the amplitude of, e.g., temperature fluctuations can be significantly larger than those in the shallow littoral zone.

Measurements—Lake Constance is one of the largest lakes in Central Europe (Fig. 1a). The lake consists of two basins connected by the shallow Lake Rhine: the deep main basin Upper Lake Constance (63 km long, 14 km wide) is located upstream of the shallower basin, called Lower Lake Constance. The central part of Upper Lake Constance has a maximum depth of 252 m and a mean depth of 101 m. Its subbasin Lake Überlingen (maximum and mean depths are 147 m and 84 m, respectively) is separated from the central part of Upper Lake Constance by the Mainau Sill reaching up to 100 m water depth (Wessels 1998). For general information on the hydrodynamics of Upper Lake Constance, *see* Bäuerle et al. (1998).

This study concentrates on data from two different moorings deployed in Upper Lake Constance: Mooring M1, located at 147 m depth in the deepest part of Lake Überlingen (Fig. 1a), measures meteorological parameters at the surface and water temperature at 34 depth levels with a fast-response thermistor chain (Precision Measurement Engineering) at a sampling interval of 60 s. The mooring has been operated continuously since December 2003.

Mooring M2 was deployed nearshore (about 75 m offshore) from June to December 2004 at a depth of 19 m. Its location was near the intersection between Lake Überlingen and the central basin of Upper Lake Constance (Fig. 1a). M2 consisted of a 500-kHz acoustic Doppler current profiler (NDP, Nortek AS) in combination with five individual temperature loggers (TR-1050, RBR Ltd.) at depths of 19, 18, 15, 11, and 7 m. The sampling interval of the thermistors was set to 10 s (the nominal response time of the TR-1050 thermistors is less than 3 s). Two additional TR-1050 temperature loggers were deployed further upslope from mooring M2 at 7 and 3 m depth (at a local depth of 7 m) from 08 July to 20 August 2004 (Fig. 1b).

The upward-looking NDP at mooring M2 was deployed in a gimbal mount at a depth of 18.5 m (Fig. 1b). It was operated in pulse-coherent mode and was connected to an onshore computer and power supply. The sampling interval was 1 s, and 10 individual profiles were averaged internally before the data were recorded on the computer, resulting in a profile interval of 10 s. The vertical bin size was 13 cm, and data were recorded for 64 bins, resulting in a measured depth range from 1.33 to 9.52 m above the sediment (17.7- to 9.5-m depth). The NDP was mounted vertically with typical pitch and roll angles of less than $\pm 3^{\circ}$. The vertical velocity refers to a Cartesian (earth) coordinate system. The bottom slope at the deployment site, however, was very steep (approximately 35°) so that the vertical coordinate is locally not perpendicular to the sediment surface. The horizontal velocities were rotated in a horizontal plane to represent cross-slope and along-slope current velocities. The NDP data were contaminated by singular spikes, the frequency of occurrence of which increased with increasing distance from the instrument. These spikes were removed, and the remaining data were averaged into 1-min samples for the subsequent analysis in order to avoid data gaps or interpolations. Continuous time series of the 1-min samples, however, could only be obtained from the depth cell closest to the instrument (at a depth of 17.7). Hence, the following time series analysis will be restricted to data from the deepest cell.

Observations—The temperature time series measured at the nearshore mooring M2 at a 15-m depth is shown in Fig. 2a. Temperature increases during summer (June to end of September), and declines during autumn and winter when wind mixing and surface-layer convection penetrates down to the depth of the measurements. The most striking feature of the time series in Fig. 2, however, is the very strong temperature variance during summer, which ceases during autumn and winter. Most of this variance occurs during particular events, as exemplified in Fig. 2b, which shows the large amplitudes of these fluctuations. During summer, the temperature frequently fluctuates between the mean summer and mean winter temperature on timescales

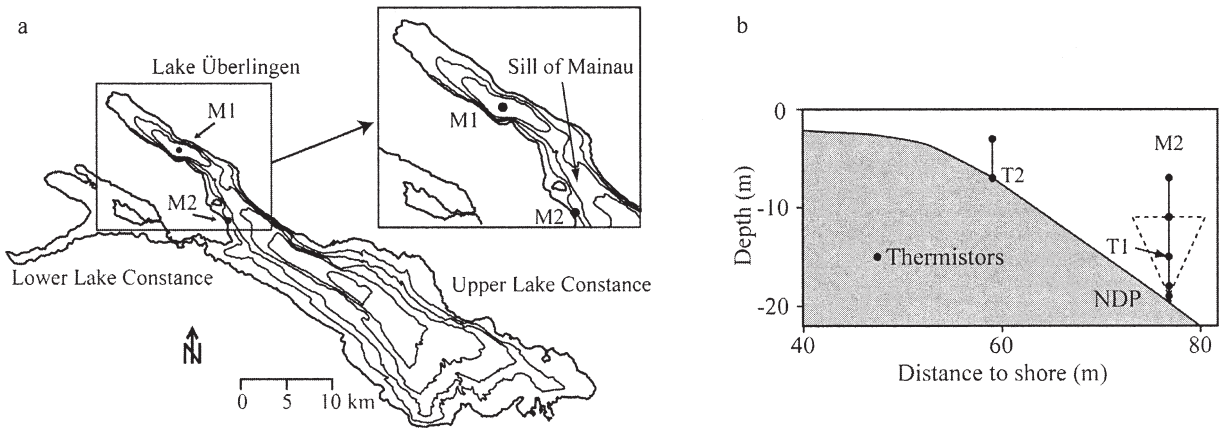

Fig. 1. (a) Lake Constance (47°83′99N, 9°81′89E) bathymetry with locations of the moorings M1 (central Lake Überlingen) and M2 (nearshore mooring between Upper Lake Constance and Lake Überlingen). The contour lines represent isobaths with an increment of 50 m. (Original map courtesy of Martin Wessels.) (b) Details of mooring M2 showing the locations and depths of the temperature loggers and the Nortek Doppler Profiler (NDP) relative to the bottom slope (figure is to scale). The thermistors at M2 were deployed straight above the NDP and the dashed lines indicate the profiling range and the beam spreading of the NDP.

of minutes. The temperature change at a 15-m depth can be as high as 7°C, and it is usually periodic, with time periods between 10 and 20 min (Fig. 2b). Temperature fluctuations with similar time periods and amplitudes were also frequently observed immediately above the sediment at a local depth of 7 m (Fig. 2b).

These temperature data reveal that organisms living in the deeper littoral zone have to cope with large temperature variations on very short timescales. The large amplitude high-frequency temperature fluctuations may significantly contribute to stress of juvenile fish or affect growth rates of sessile species sensitive to temperature. Temperature was shown to be an important environmental factor controlling the diapause termination in zooplankton (e.g., Pfrender and Deng 1998) or the distribution and habitat preference of fish (Hofmann and Fischer 2002; Wacker 2005; both studies were performed in the littoral zone of Lake Constance).

The temperature fluctuations discussed above are associated with periodic current velocity fluctuations with

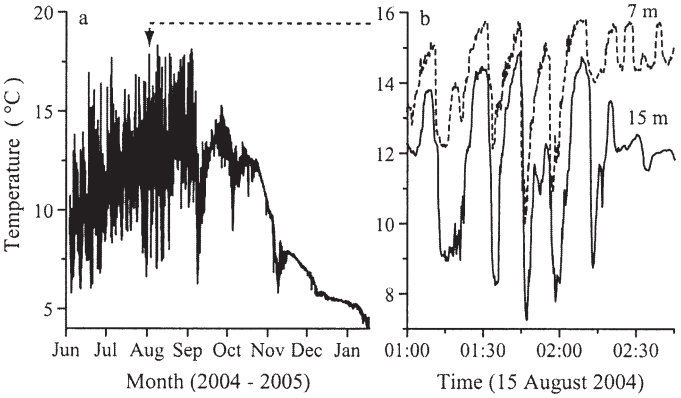

Fig. 2. (a) Temperature time series measured at the nearshore mooring M2 at a depth of 15 m. (b) Subsection of the entire time series, emphasizing the dynamics and the details of the strong temperature fluctuations. In addition to the temperature at a 15-m depth (on mooring M2), it shows the temperature measured 10 cm above the bottom at a local depth of 7 m (dashed line).

amplitudes of up to 10 cm s^{-1}. The power spectra of the velocity fluctuations shown in Fig. 3 demonstrate that the high-frequency current fluctuations contribute a significant part of the total kinetic energy available in the deeper littoral zone. Although the spectrum of the along-shore velocity component only has a shoulder in the high-frequency range, the spectra of the across-shore and vertical velocities show a clear peak around a frequency corresponding to a period of ~10 min. In case of the vertical velocity component, this peak represents the maximum spectral energy within the considered range of frequencies. The highest spectral energy in the low-frequency range could be observed in the along-shore velocity component. All three velocity components have another, more confined, spectral peak at 2.5 10^{-5} Hz (all frequencies are given in cyclic units), corresponding to a period around 11 h. This spectral peak can be most probably attributed to the first mode Poincaré-type internal oscillation, which exhibits one well-developed, anticyclonically rotating amphidromic system in the central basin of Upper Lake Constance (Bäuerle et al. 1998; Wang et al. 2000). No enhanced spectral energy, however, could be observed at the corresponding frequency of the dominant basin-scale Kelvin wave in Lake Constance ($f \approx 3.1 \times 10^{-6}$ Hz, Appt et al. 2004). However, the spectral resolution at these low frequencies is rather poor. Temperature spectra from M1 and M2 (Fig. 3c) look very similar to the spectrum of the along-shore current velocity, and they do not show any significant differences besides a slightly enhanced spectral energy within the internal wave band at the nearshore Sta. M2. The absence of a clear spectral peak in the temperature spectra, as well as in the spectrum of the along-shore velocity component, can be attributed to the general "red" behavior of these spectra, which leads to a partial masking of the peak by the strong increase of spectral power towards lower frequencies.

In accordance with numerous observations in lakes (e.g., Thorpe et al. 1996; Stevens 1999; Antenucci and Imberger 2001) as well as in the ocean (Dillon and Caldwell 1980;

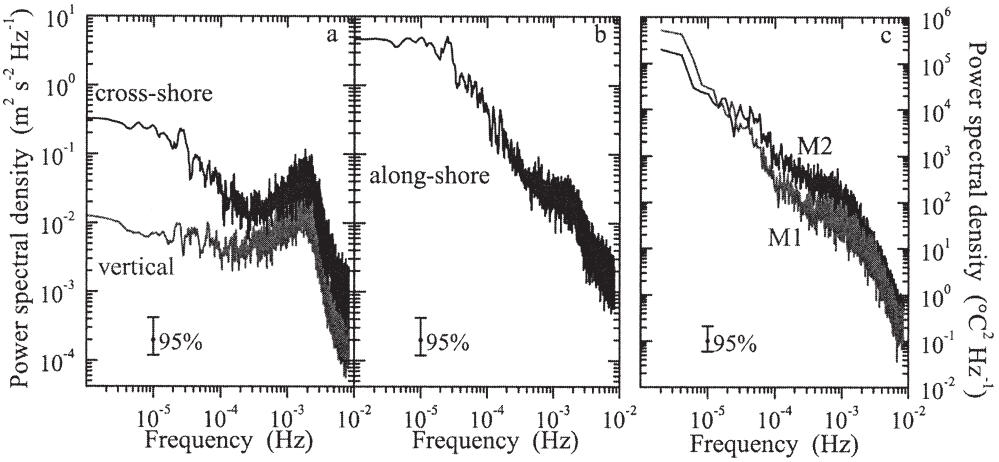

Fig. 3. Power spectra of the (a) cross-shore and vertical, and (b) along-shore current velocities measured at M1 at a 17.7-m depth, as well as (c) temperatures measured at M1 and M2 at 18.4- and 17.7-m depths, respectively. The spectra were estimated for the time period from 07 July to 08 August 2004.

Eriksen 1982; Van Haren et al. 1994), the observed periodic fluctuations in temperature and in the current velocity can be attributed to internal waves. To investigate the temporal dynamics of these propagating internal waves, the spectral analysis was applied to half-overlapping subsections of the current velocity time series such that each spectrum covered a time period of 8.5 h. The temporal evolution of the vertical velocity fluctuation spectra at the nearshore mooring M1 at a depth of 17.7 m (1.3 m above the sediment) is shown in Fig. 4. The seasonal dynamics of the spectral energy in the velocity fluctuations at time periods between 10 and 15 min reproduces approximately the observed temporal evolution of the variance in the temperature measurements from Fig. 2. High-frequency internal waves with periods between 10 and 15 min could be observed from July until the end of September. During this time period, the high-frequency internal waves accounted for the major part of the energy contained in the vertical velocity fluctuations.

The existence of propagating internal waves in unbounded water bodies is restricted to the frequency range between the inertial frequency and the buoyancy frequency N (Garrett and Munk 1972), with

$$N^2 = \frac{g}{\rho}\frac{\partial \rho}{\partial z} \quad (1)$$

(g denotes gravitational acceleration, ρ density, and z depth [increasing toward the bottom]). Numerous observations, however, have shown that most of the spectral energy of high-frequency internal waves can be found near their high-frequency limit N (Thorpe et al. 1996; Saggio and Imberger 1998; Boegman et al. 2003). The corresponding buoyancy period $2\pi/N$ was estimated from the temperature profiles measured at mooring M2 and added to the contour plot in Fig. 4 (N^2 was estimated from the temperature differences between neighbored thermistors; a running average over 7 h was applied before the calculation). Within the stratified period, the frequency associated with the peak in the energy spectrum is near N (Fig. 4), which follows the above-cited observations. The sudden increase in buoyancy period on 15 August and on 24 September were caused by strong wind events, leading to a broadband excitation of the velocity spectrum and to vertical mixing (decreasing N). During November and December, the spectral energy within the high-frequency range of the spectrum is significantly reduced compared with the summer months,

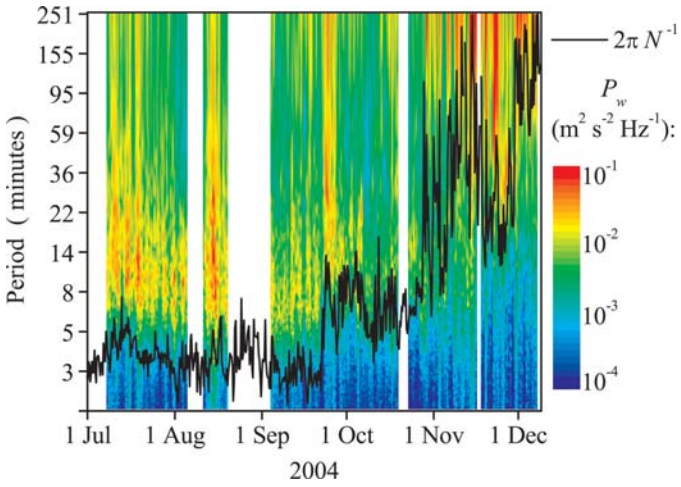

Fig. 4. Contour plot of the power-spectral density of the vertical component of the current velocity (measured at M2 at a 17.7-m depth) as a function of time. The vertical axis shows the respective time periods T associated with the corresponding frequencies f of the spectral analysis ($T = 1/f$). The different colors refer to power spectral density (white denotes missing data). The black line shows the buoyancy period ($T = 2\pi/N$) as estimated from the thermistor string at mooring M2 at a depth of 15.5 m. Two major wind events, with wind speeds exceeding 8 m s^{-1}, are marked by arrows on top of the graph.

and the energy contained in the low frequencies, with periods exceeding 30 min, is strongly increased.

Discussion—The observations reveal that high-frequency internal waves are not only a feature of the open water column, but also that they can dominantly contribute to the temperature and current velocity variance in the littoral zone. Given the potential ecological consequences of such strong fluctuations, the question about the timing and the frequency of occurrence of internal wave activity near the lake boundaries and in the littoral zone becomes important.

The interaction of high-frequency internal waves with sloping topography received increasing attention during the last decades due to its potential significance for basin-wide diapycnal mixing in the ocean and as well as in lakes (Munk 1966; Imberger 1998). The reflection of internal waves at frequencies close to the critical frequency

$$f_c = \frac{1}{2\pi}\left(N^2 \sin^2 \alpha + f_i^2 \cos^2 \alpha\right)^{1/2}.$$

where α is the angle that the slope makes to the horizontal and f_i the inertial frequency, may lead to turbulent mixing in the sloping boundary layer (Eriksen 1985; Ivey and Nokes 1989). Neglecting the effect of earth's rotation and using $\alpha = 35^\circ$ (Fig. 1b) and an average buoyancy frequency of $N^2 = 4 \times 10^{-4}$ s^{-2}, as was estimated at M2 at a depth of 11 m for the period from 07 July to 08 August 2004 (Fig. 4), results in a critical frequency of $f_c \approx 2 \times 10^{-3}$ Hz (in cyclic units), corresponding to a period of $T_c \approx 9$ min.

Thus, following Eriksen (1982, 1998), the observed enhancement of spectral energy at this frequency or period in the velocity spectra (Figs. 3 and 4) may be attributed to the critical reflection of internal waves at the local bottom slope. Because critical reflection of internal waves results in a wave-number vector that is parallel to the bottom, the enhancement of spectral energy should be confined to the bottom boundary layer. The temperature spectra measured near- and offshore (at M2 and M1, respectively, Fig. 3), however, reveal only a slight difference in spectral energy in the frequency band near the critical frequency at our nearshore site. Hence, whether wave reflection at the critical angle contributes significantly to the observed spectral energy of the high-frequency internal waves nearshore cannot be decided on the basis of our temperature data but requires offshore measurements of the current velocity.

Many possible mechanisms capable of generating high-frequency internal waves have been suggested in the literature (e.g., Boegman et al. 2003, and references therein). The radiation of high-frequency internal waves from steepened basin-scale oscillations (Thorpe et al. 1996; Horn et al. 2001) or the interaction of basin-scale oscillations with the lake topography (Imberger 1994; Thorpe et al. 1996) are only two of these. To investigate the linkage between the observation of high-frequency internal waves in the nearshore zone and basin-scale oscillations, the cross-correlation between the temperature at mooring M1 (Fig. 5a) and the spectral energy of the vertical velocity fluctuations at mooring M2 was calculated. In this cross-correlation, we used the observed temperature at a fixed depth instead of isotherm depth to enable a comparison of the temperature data from M1 with the current velocity measurements from a fixed depth at Sta. M2. Moreover, the depths of the isotherms changed during the observation period as a result of seasonal warming and thus are not appropriate for a long-term comparison with the current velocity data. The cross-correlation was estimated between the temperature at M1 at a depth of 18.4 m and the spectral energy of the vertical velocity fluctuations at a fixed frequency (1.94×10^{-3} Hz, corresponding to a period of 9 min) measured at M2 at a depth of 17.7 m (1.3 m above the sediment). It is evident from Fig. 5b that the cross-correlation is a periodic function with a period of about 4 d, the period of the dominant internal Kelvin wave in Lake Constance (Bäuerle et al. 1998; Appt et al. 2004).

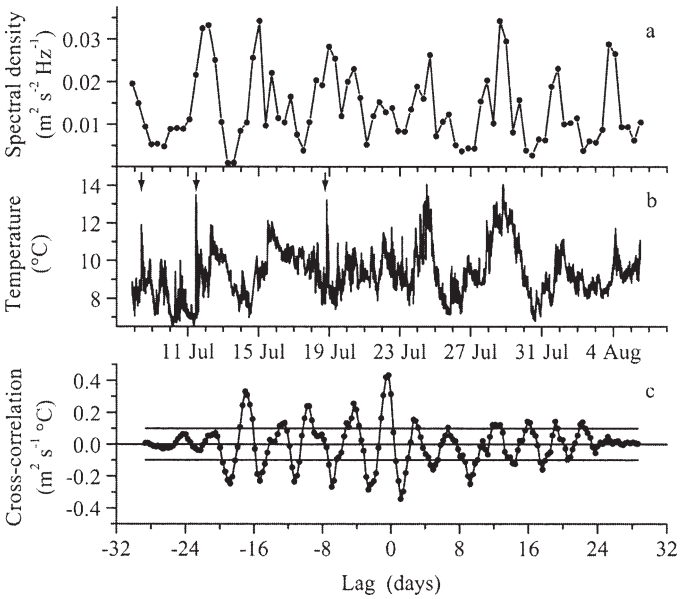

Fig. 5. (a) Time series of the power spectral density of the vertical component of the current velocity measured at M2 (17.7 m depth) between 07 July and 08 August 2004 at a frequency of 1.94×10^{-3} Hz (corresponding to a period of 9 min, see Fig. 4). (b) Temperature recorded at mooring M1 at a depth of 18.4 m. The arrows on top of the graph indicate large-amplitude high-frequency internal wave events as they were exemplified in Fig. 2b. (c) Cross-correlation between the time series shown in (a) and (b), respectively. The cross-correlation was estimated for the time period from 07 July to 08 August 2004. The dashed lines indicate the approximated standard error of the correlation coefficient because it was estimated under the hypothesis that both time series are uncorrelated.

This periodic cross-correlation function suggests a strong coupling between the basin-scale Kelvin wave and the occurrence of high-frequency internal waves at the nearshore Sta. M2. The positive peak near the zero lag further suggests that higher temperature (downwelling) at the central mooring M1 coincided with the observations of internal wave activity at M2. Unfortunately, we do not know the direction of propagation of the high-frequency internal waves. According to Thorpe and Umlauf (2002),

such information cannot be inferred from single-point measurements on steep slopes with vertically varying buoyancy frequencies. No conclusive insight into the nature of the coupling mechanism between the basin-scale and the high-frequency internal waves can be obtained without such information. The origin of the high-frequency waves can be offshore, where nonlinear steepening or the interaction of the basin-scale Kelvin wave with the topography of the lake (e.g., with the Sill of Mainau, Fig. 1a) can lead to the generation of propagating high-frequency waves. Alternatively, the origin of the high-frequency waves can be near shore, and the observations at mooring M2 show locally generated internal waves, produced by the interaction of the Kelvin wave with the steep slope at the measurement site. Future experiments will aim on the estimation of directional wave spectra of internal waves on the slope in order to calculate their phase relations with the basin-scale Kelvin wave. Such data will provide a basis to investigate mechanistic theories about the coupling mechanism between basin-scale oscillations and high-frequency internal waves in the nearshore region.

To summarize, high-frequency internal waves are the physical process dominating the variability of the current field in the deeper littoral zone. In addition to strong current velocity fluctuations, high-frequency internal waves cause very large temperature fluctuations with periods around the buoyancy frequency. These temperature fluctuations in particular can be assumed to play an important role in the ecology of the littoral zone.

Andreas Lorke[1]
Frank Peeters

Environmental Physics
Limnological Institute
University of Konstanz
Mainaustrasse 252
D-78464 Konstanz, Germany

Erich Bäuerle

Wasseransichten Moislingen
D-21369 Nahrendorf
Germany

References

Antenucci, J. P., and J. Imberger. 2001. On internal waves near the high-frequency limit in an enclosed basin. J. Geophys. Res. **106:** 22465–22474.

Appt, J., J. Imberger, and H. Kobus. 2004. Basin-scale motion in stratified Upper Lake Constance. Limnol. Oceanogr. **49:** 919–933.

[1] Corresponding author (Andreas.Lorke@uni-konstanz.de).

Acknowledgments

We thank B. Rosenberg and J. Halder for their help in the field. The radio link to the data buoy was made possible by O. Kotheimer and the School Salem Castle. D. McGinnis and two anonymous reviewers provided helpful comments on the manuscript. The work was financially supported by the German Research Foundation within the framework of the Collaborative Research Center 454: The littoral zone of Lake Constance.

Bäuerle, E., D. Ollinger, and J. Ilmberger. 1998. Some meteorological, hydrological, and hydrodynamical aspects of Upper Lake Constance. Arch. Hydrobiol. Spec. Issues Adv. Limnol. **53:** 31–83.

Boegman, L., J. Imberger, G. N. Ivey, and J. P. Antenucci. 2003. High-frequency internal waves in large stratified lakes. Limnol. Oceanogr. **48:** 895–919.

Dillon, T. M., and D. R. Caldwell. 1980. High-frequency internal waves at ocean station P. J. Geophys. Res. **85:** 3277–3284.

Eriksen, C. C. 1982. Observations of internal wave reflection off sloping boundaries. J. Geophys. Res. **87:** 525–538.

———. 1985. Implications of ocean bottom reflection for internal wave spectra and mixing. J. Phys. Oceanogr. **15:** 1145–1156.

———. 1998. Internal wave reflection and mixing at Fieberling Guyot. J. Geophys. Res. **103:** 2977–2994.

Garrett, C., and W. Munk. 1972. Space-time scales of internal waves. Geophys. Fluid Dyn. **2:** 225–264.

Hofmann, N., and P. Fischer. 2002. Temperature preferences and critical thermal limits of burbot: Implications for habitat selection and ontogenetic habitat shift. Trans. Am. Fish. Soc. **131:** 1164–1172.

Horn, D. A., J. Imberger, and G. N. Ivey. 2001. The degeneration of large-scale interfacial gravity waves in lakes. J. Fluid Mech. **434:** 181–207.

Imberger, J. 1994. Transport processes in lakes: A review, p. 99–193. *In* R. Margalef [ed.], Limnology Now. Elsevier.

———. 1998. Flux paths in a stratified lake: A review, p. 1–18. *In* J. Imberger [ed.], Physical processes in lakes and oceans. Coastal and Estuarine Studies. American Geophysical Union.

Ivey, G. N., and R. I. Nokes. 1989. Vertical mixing due to the breaking of critical internal waves on sloping boundaries. J. Fluid Mech. **204:** 479–500.

Munk, W. 1966. Abyssal recipes. Deep-Sea Res. **13:** 707–730.

Pfrender, M. E., and H. W. Deng. 1998. Environmental and genetic control of diapause termination in *Daphnia*. Arch. Hydrobiol. Spec. Issues Adv. Limnol. **52:** 237–251.

Saggio, A., and J. Imberger. 1998. Internal wave weather in a stratified lake. Limnol. Oceanogr. **43:** 1780–1795.

Stevens, C. L. 1999. Internal waves in a small reservoir. J. Geophys. Res. **104:** 15777–15788.

Thorpe, S. A., J. M. Keen, R. Jiang, and U. Lemmin. 1996. High-frequency internal waves in Lake Geneva. Phil. Trans. R. Soc. Lond. A **354:** 237–257.

———, and L. Umlauf. 2002. Internal gravity wave frequencies and wavenumbers from single point measurements over a slope. J. Mar. Res. **60:** 699–723.

van Haren, H., N. S. Oakey, and C. Garrett. 1994. Measurements of internal wave band eddy fluxes above a sloping boundary. J. Mar. Res. **52:** 909–946.

Wacker, N. 2005. Temporal pattern of burbot (*Lota lota* L.) in Lake Constance and environmental factors triggering the ontogenetic habitat shift of juveniles. Hartung-Gorre Verlag Konstanz.

Wang, Y., K. Hutter, and E. Bäuerle. 2000. Wind-induced baroclinic response of Lake Constance. Ann. Geophys. **18:** 1488–1501.

Wessels, M. 1998. Geological history of the Lake Constance area. Arch. Hydrobiol. Spec. Issues Adv. Limnol. **53:** 1–12.

Received: 4 August 2005
Accepted: 10 January 2006
Amended: 24 January 2006